Interlayer dependent polarity of magnetoresistance in graphene spin valves

M. Z. Iqbal[1], M. W. Iqbal[1], Xiaozhan Jin[2], Changyong Hwang[2], Jonghwa Eom[1]*

[1]Department of Physics and Graphene Research Institute, Sejong University, Seoul 143-747, Korea

[2]Center for Nanometrology, Korea Research Institute of Standards and Science, Daejeon 305-340, Korea

* Corresponding author: eom@sejong.ac.kr

We fabricated spin valves of NiFe/Al_2O_3/single layer graphene (SLG)/Co, NiFe/SLG/Co, and NiFe/Al_2O_3/Co. In the fabrication lithography processes using e-beam resist or photoresist were avoided to obtain residue-free clean junctions in all devices. While all three types of magnetic junction showed a distinctly clear spin valve effect from 10 to 300 K, the polarity of magnetoresistance (MR) revealed different signs. Negative MR (-1.6% at 10 K) was observed in the spin valve effect for the junction with the Al_2O_3/SLG interlayer, however other type of junctions showed conventional positive MR values. The positive or negative MR signs are explained within the Julliere model of spin-dependent tunneling.

1. Introduction

Graphene has been widely investigated in the field of electronic transport, but the main focus has been on lateral transport. Recently researchers have turned their attention to the vertical transport structure or junctions for graphene-based device applications. Spin transport in graphene was also studied initially in lateral transport structures.[1, 2] Although very long spin coherence was expected in carbon-based materials because of weak spin–orbit and hyperfine interactions,[3] the experiments revealed spin diffusion lengths of only a few micrometers in Si/SiO_2 substrates.[1, 2] Although recently it has been estimated that the spin diffusion length of graphene in the lateral transport structure may exceed 100 μm when prepared on hexagonal SiC substrates,[4] a feasible approach to spintronic device applications is strongly needed. A junction is a structure that is simple to fabricate and is ideally zero-dimensional, so that the size of the device can be quite small. As the lateral channel does not exist conceptually in the junction, the limitation set by the spin diffusion length cannot be an obstacle for spintronic devices in the structure of the junction.

The principal structure of a spin valve consists of two ferromagnetic metal electrodes decoupled via a nonmagnetic spacer, which permits parallel or antiparallel alignment of the magnetization of two ferromagnetic electrodes controlled by the external magnetic field. A fascinating spin filtering effect was theoretically predicted in Co/graphene/Co or Ni/graphene/Ni junctions where the Co and Ni films have (111) fcc or (0001) hcp crystal structures,[5, 6] Because of the absence of majority spin states around the K point at the Fermi level, only minority spin states from the transition-metal ferromagnetic films can contribute to transmittance through graphene. Therefore, 100% spin polarization can be produced when electrons from the ferromagnetic electrode pass through graphene. Several groups have reported on experimental studies of vertical spin valves consisting of single or bilayer

graphene and some studies showed that graphene is used to inject spins into Si.[7] However, the spin valve effect for some devices revealed positive magnetoresistance (MR) values for graphene interlayer junction,[8-13] and recently our group has reported the spin valve effect with negative MR on exfoliated single layer graphene (SLG) with Co/SLG/Al$_2$O$_3$/Ni configuration. We found less than a -0.4% MR ratio at room temperature and the spin valve signal showed relatively non-uniform plateaus.[14]

Here, we present a detail investigation of vertical spin valve which consists of three different interlayers between NiFe and Co electrodes. We have observed the clear spin valve signals with uniform plateaus in all junctions. The first type of junction had an interlayer of 1-nm-thick Al$_2$O$_3$ film and graphene (NiFe/Al$_2$O$_3$/SLG/Co) with MR values (–0.53% at 300 K to –1.6% at 10 K), the second had an interlayer of graphene (NiFe/SLG/Co) having magnitude of MR (0.15% at 300 K to 0.23% at 10 K) and the third had a 1-nm-thick Al$_2$O$_3$ film as interlayer (NiFe/Al$_2$O$_3$/Co), of MR (0.33% at 300 K to 0.76% at 10 K). The linear I–V characteristic of NiFe/SLG/Co junction is an indicative of Ohmic properties, while the junctions with NiFe/Al$_2$O$_3$/SLG/Co and NiFe/Al$_2$O$_3$/Co interlayers showed nonlinear I–V characteristics which indicates the tunneling properties. The results revealed that NiFe/Al$_2$O$_3$/SLG/Co junction exhibit negative MR while the NiFe/SLG/Co and NiFe/Al$_2$O$_3$/Co showed positive MR values at different temperatures. We explained the MR switching mechanism from the comparative analysis of these three junctions.

2. Experimental

2.1. Material and device fabrication

The graphene film in this experiment was grown on 25-μm-thick copper foils from Alfa Aesar (99.8% pure) via thermal chemical vapor deposition (CVD). A mechanically polished

and an electropolished copper foil were inserted into a thermal CVD furnace. The furnace was evacuated to ~10^{-4} Torr, and the temperature rose to 1010 °C with H_2 gas flow (~10^{-2} Torr). After the temperature became stable at 1010 °C, both CH_4 (20 standard cubic centimeters per minute (sccm)) and H_2 (5 sccm) were injected into the furnace to synthesize the graphene for 8 min. After graphene synthesis, the sample was cooled at a rate of 50 °C/min to room temperature [15-18]. The graphene film grown on Cu foil was transferred to a Si/SiO_2 substrate with the wet transfer method. Prior to wet etching, the surface of the graphene was spin-coated with poly(methyl methacrylate) (PMMA), and then baked at 150 °C for 3 min. The purpose of the PMMA coating was to protect the graphene films from cracking and breaking during the transfer process. The bottom Cu foil was removed by etching in 1 M solution of ammonium persulfate ((NH_4)$_2S_2O_8$), and the PMMA membrane was washed with deionized water. Next, the graphene films with PMMA membrane were transferred onto Si/SiO_2 substrates, where the bottom NiFe electrodes had already been prepared using metal masks. The residual PMMA film was dissolved and removed with acetone.[15] The device fabrication was divided into processes for three different parts: the bottom NiFe film, graphene, and the top Co film. Initially, the bottom NiFe electrodes (30 nm thick) were patterned on the Si substrate with a 300-nm-thick SiO_2 cap layer by using metal masks. After removing the metal mask, a thin (1-nm) layer of Al_2O_3 was deposited using atomic layer deposition (ALD). Lucida™ D series NCD water-based ALD with trimethylaluminum (TMA) precursor is used for the growth of Al_2O_3 film. During the growth of Al_2O_3 film, the chamber pressure was kept 1.3 Torr and substrate temperature was kept 120 °C. Next, a single layer of graphene was transferred to cover the entire surface on the bottom NiFe electrodes. Subsequently, the top Co electrodes (55 nm thick) were patterned by using metal masks. Lithography processes using e-beam resist or photoresist were avoided to obtain residue-free clean junctions in all devices.

2.2. Device characterization and measurement setup

The quality of graphene was determined using Renishaw Raman spectroscopy with 514 nm excitation. After analyzing the properties of graphene, unnecessary graphene was removed by using O_2 plasma etching (except underneath the Co electrode). The removal of unnecessary graphene was essential to avoid bypass current outside the junction. The electrical and magnetotransport properties of graphene junctions were measured using AC lock-in techniques at 11.7 Hz with the root-mean-square current amplitude of 50 μA. Low temperature measurements were carried out in a liquid He cryostat. A Lake Shore 331 temperature controller was used to modulate and control the temperature range.

3. Results and discussion

3.1. Characterization of graphene spin valve devices

Figure 1a shows a schematic of the spin valve consisting of a top Co electrode (FM1), a bottom NiFe electrode (FM2), a graphene interlayer, and an Al_2O_3 layer. The optical micrograph image of a complete device structure is shown in Figure 1b. The width of FM1 and FM2 was 70 and 100 μm, respectively. The other two sets of devices with the same configuration were made using a graphene and Al_2O_3 interlayer separately. The in-plane magnetic field (H) was applied at 45° to the direction of the ferromagnetic (FM) electrodes. As the switching magnetic fields of the Co and NiFe films are different, the magnetization can be aligned parallel or antiparallel by sweeping H. The probe configuration for MR measurement of the junction is depicted in Figure 1b. The Raman spectra of graphene on SiO_2 and ferromagnetic electrodes are shown in Figure 1c. The full width at half maximum (FWHM) of the 2D band was about 30 cm^{-1} and the 2D/G peak intensity ratio was ~3.51 and

4.02 for graphene/SiO_2 and NiFe electrode, respectively, indicating a single layer of graphene.[19] Unlike for mechanically exfoliated graphene, there are usually defects or vacancies present along the catalyst boundaries generated during growth in CVD graphene. However, the D-peak intensity in the Raman spectra of graphene indicated a defect density of graphene film on NiFe electrode.

We have performed atomic force microscopy (AFM) to observe the surface morphology of the Al_2O_3 film. Figure 2a shows the AFM image of NiFe electrode before Al_2O_3 deposition, where the surface was smooth and uniform. The AFM image of the NiFe surface after deposition of 1-nm-thick Al_2O_3 is shown in Fig. 2b. The non-uniform surface can be easily seen and pinholes are also observed in the certain regions highlighted by white rectangles in Figure 2c,d. The pinholes make leakage current through the junction and reduce the spin valve signals.

3.2. Current-voltage characteristics and temperature dependent resistance-area product

The I–V characteristics of the junctions were investigated and are shown in Figure 3a for the single layer graphene (black line), Al_2O_3 (blue line), and Al_2O_3/graphene (red line) interlayer junctions. The graphene interlayer junction showed a linear I–V curve indicative of Ohmic behavior,[10, 12] whereas the Al_2O_3/graphene and Al_2O_3 junctions showed nonlinear I–V curves corresponding to tunneling characteristics.[14, 20] These results were further verified by measuring the junction resistance (R) of these devices as a function of temperature in the parallel magnetization configuration. Figure 3b shows the resistance-area product (RA), i.e., the product of R and the junction area (A) as a function of temperature for the

Al$_2$O$_3$/graphene interlayer junction. The RA monotonically increases as the temperature is lowered, which supports the idea that the junction is in the tunneling regime. The RA of the Al$_2$O$_3$ interlayer junction also shows similar temperature dependence (Figure 3d). The Al$_2$O$_3$ interlayer junction is confirmed to be in the tunneling regime, as is the case for an insulating layer between ferromagnetic electrodes in conventional TMR devices.[21] However, the graphene interlayer junction shows a distinctively different characteristic with temperature. The RA decreases with decreasing temperature (Figure 3c), which confirms that the graphene interlayer junction has Ohmic behavior. The behavior with temperature of the graphene interlayer junction was attributed to the inelastic scattering with phonons similar to that in a metallic layer, while the behavior of the Al$_2$O$_3$/graphene or Al$_2$O$_3$ interlayer junctions with temperature is caused by the transmittance of the tunneling barrier.

3.3. Spin valve effect in graphene, Al$_2$O$_3$, and Al$_2$O$_3$/graphene devices

The MR ratio, which is defined as MR = [R(H) − R$_P$]/R$_P$ was used to study the spin valve effect. Here, R(H) is the magnetic field-dependent resistance and R$_P$ is the resistance corresponding to the parallel alignment of the magnetization. Figure 4a shows MR for the junction made of Al$_2$O$_3$/graphene interlayer at temperatures from 10 K to 300 K. This junction shows negative MR where high (low) resistance appears in the parallel (antiparallel) magnetization configuration between FM1 and FM2. The MR values for this junction increased from –0.53% at 300 K to –1.6% at 10 K. Dlubak et al. observed higher MR at low temperature (1.4 K) of the same device structure which may be due to the direct growth of graphene on nickel film but lower than to the theoretical predication may be due to disorder or roughness of metals and graphene interface.[5, 6, 22] However, the MR in this experiment is larger than recently reported value at RT.[14] For comparison we also measured the MR for NiFe/SLG/Co and NiFe/Al$_2$O$_3$/Co junctions. The NiFe/SLG/Co junction showed a positive

7

MR signal with magnitude increased from 0.15% at 300 K to 0.23% at 10 K (Figure 4b) and

MR for the NiFe/Al$_2$O$_3$/Co junction also exhibit positive MR increased from 0.33% at 300 K

to 0.76% at 10 K (Figure 4c).

Although these results show the characteristic features of three types of junctions having

different interlayers with negative or positive MR values. Nevertheless, the MR of the

NiFe/Al$_2$O$_3$/Co junction which is relatively lower than the standard value. The MR value

specifically depends on junction interface and uniformity of the oxide layer. The formation of

high quality Al$_2$O$_3$ tunnel barrier without pinholes is challenging. The surface non-uniformity

definitely affects the performance of the device and reduces the value of spin signal. The

junction area of our devices are 70x100 μm^2. For such a large junction area, the surface

roughness and a number of regions with pinholes can be observed as shown in Figure 2c,d.

Thus the lower value of MR may be due to defects and pinholes in the large junction.[23]

The surface of NiFe electrode can be also affected by graphene transfer process. Graphene

transfer on NiFe electrodes occurs in air and use of wet chemistry. The exposure to air

certainly oxidizes the NiFe electrode surface and some of chemical residue retains on the

graphene surface. The observed defect peak in Raman spectra indicates the existence of the

chemical residue on the graphene surface (see Figure 1c). These processes definitely decrease

the MR values.

3.4. Interpretation of the MR sign of Al$_2$O$_3$/graphene junction

A positive or negative MR value is expected for the spin valve effect and it can be elucidated with the well-established Julliere model of spin dependent tunneling and the recent review.[24, 25] The MR can be written as $2 x P_1 x P_2/(1-P_1 x P_2)$ with P_1 and P_2 being the effective spin polarization of ferromagnet (FM) electrode interfaces. In the first approximation MR is proportional to $P_1 x P_2$, and this product drives the MR sign. Here, taking P_G as the spin polarization of the FM/graphene interface and P_A as the spin polarization of the FM/Al$_2$O$_3$ interface, we can analyze the measured MR signals as follows: Figure 4a gives $P_G x P_A < 0$, Figure 4b gives $P_G x P_G > 0$ and Fig. 4c gives $P_A x P_A > 0$. The results of Figure 4b,c are well expected as these junctions are almost symmetrical except for the materials of ferromagnetic electrodes. Since the product of $P_G x P_A$ is negative, one of P_G or P_A must be negative. The polarization P_A of the FM/Al$_2$O$_3$ is known to be positive.[25] Therefore P_G should be negative, confirming the reversal of spin polarization at the FM/graphene interface. Following this interpretation by the Julliere model we can understand the positive magnetoresistance observed in FM/graphene/FM junctions. Since spin-filtering happens at both interfaces, we still expect the *MR* sign (= $P_G x P_G$) positive.

4. Conclusion

In conclusion, we have demonstrated the spin valve effect in NiFe and Co junctions with Al$_2$O$_3$/graphene, graphene, and Al$_2$O$_3$ interlayers. While the graphene interlayer junction revealed a linear I–V curve indicating that the Ohmic property was dominant, the Al$_2$O$_3$/graphene and Al$_2$O$_3$ interlayer junctions showed nonlinear I–V curves that correspond to tunneling characteristics. The NiFe/Al$_2$O$_3$/SLG/Co junction showed a negative MR signal –0.53% at room temperature. The MR showed a distinctly clear signal with uniform plateaus, and increased up to –1.6% at 10 K. Other types of junctions such as NiFe/SLG/Co and NiFe/Al$_2$O$_3$/Co revealed positive MR signals. The spin valve effect was perceived to retain

the spin-polarized transport in the vertical direction and MR values with different signs suggested distinct functionality of the interface. The positive or negative MR signs are explained within the Julliere model of spin-dependent tunneling. Using the fact that the sign of the MR value in the spin valve effect is selectable by the interlayer structure, the graphene interlayer junction is expected to be an attractive candidate for a new type of spintronic device.

Acknowledgements

References

1. N. Tombros, C. Jozsa, M. Popinciuc, H. T. Jonkman and B. J. van Wees, *Nature*, 2007, 448, 571-U574.

2. W. Han and R. K. Kawakami, *Phys Rev Lett*, 2011, 107, 047207.

3. J. Fischer, B. Trauzettel and D. Loss, *Phys Rev B*, 2009, 80, 155401.

4. B. Dlubak, M. B. Martin, C. Deranlot, B. Servet, S. Xavier, R. Mattana, M. Sprinkle, C. Berger, W. A. De Heer, F. Petroff, A. Anane, P. Seneor and A. Fert, *Nature Physics*, 2012, 8, 557-561.

5. V. M. Karpan, G. Giovannetti, P. A. Khomyakov, M. Talanana, A. A. Starikov, M. Zwierzycki, J. van den Brink, G. Brocks and P. J. Kelly, *Phys Rev Lett*, 2007, 99, 176602.

6. V. M. Karpan, P. A. Khomyakov, A. A. Starikov, G. Giovannetti, M. Zwierzycki, M. Talanana, G. Brocks, J. van den Brink and P. J. Kelly, *Phys Rev B*, 2008, 78, 195419.

7. O. Van't Erve, A. Friedman, E. Cobas, C. Li, J. Robinson and B. Jonker, *Nat Nanotechnol*, 2012, 7, 737-742.

8. J.-H. Park and H.-J. Lee, *Phys Rev B*, 2014, 89, 165417.

9. T. M. Mohiuddin, E. Hill, D. Elias, A. Zhukov, K. Novoselov and A. Geim, *Ieee T Magn*, 2008, 44, 2624.

10. M. Z. Iqbal, M. W. Iqbal, J. H. Lee, Y. S. Kim, S. H. Chun and J. Eom, *Nano Res*, 2013, 6, 373-380.

11. E. Cobas, A. L. Friedman, O. M. J. van't Erve, J. T. Robinson and B. T. Jonker, *Nano Lett*, 2012, 12, 3000-3004.

12. J. Meng, J. J. Chen, Y. Yan, D. P. Yu and Z. M. Liao, *Nanoscale*, 2013, 5, 8894-8898.

13. W. Li, L. Xue, H. Abruña and D. Ralph, *Phys Rev B*, 2014, 89, 184418.

14. A. K. Singh and J. Eom, *ACS Appl Mater Interfaces*, 2014, DOI: 10.1021/am4049145.

15. K. S. Kim, Y. Zhao, H. Jang, S. Y. Lee, J. M. Kim, K. S. Kim, J. H. Ahn, P. Kim, J. Y. Choi and B. H. Hong, *Nature*, 2009, 457, 706-710.

16. X. S. Li, Y. W. Zhu, W. W. Cai, M. Borysiak, B. Y. Han, D. Chen, R. D. Piner, L. Colombo and R. S. Ruoff, *Nano Lett*, 2009, 9, 4359-4363.

17. S. Bae, H. Kim, Y. Lee, X. F. Xu, J. S. Park, Y. Zheng, J. Balakrishnan, T. Lei, H. R. Kim, Y. I. Song, Y. J. Kim, K. S. Kim, B. Ozyilmaz, J. H. Ahn, B. H. Hong and S. Iijima, *Nat Nanotechnol*, 2010, 5, 574-578.

18. X. S. Li, C. W. Magnuson, A. Venugopal, R. M. Tromp, J. B. Hannon, E. M. Vogel, L. Colombo and R. S. Ruoff, *J Am Chem Soc*, 2011, 133, 2816-2819.

19. A. C. Ferrari, J. C. Meyer, V. Scardaci, C. Casiraghi, M. Lazzeri, F. Mauri, S. Piscanec, D. Jiang, K. S. Novoselov, S. Roth and A. K. Geim, *Phys Rev Lett*, 2006, 97, 187401.

20. I. V. Shvets, A. N. Grigorenko, K. S. Novoselov and D. J. Mapps, *Appl Phys Lett*, 2005, 86, 212501.

21. S. Yuasa and D. D. Djayaprawira, *J Phys D Appl Phys*, 2007, 40, R337-R354.

22. B. Dlubak, M. B. Martin, R. S. Weatherup, H. Yang, C. Deranlot, R. Blume, R. Schloegl, A. Fert, A. Anane, S. Hofmann, P. Seneor and J. Robertson, *Acs Nano*, 2012, 6, 10930-10934.

23. J.-J. Chen, J. Meng, Y.-B. Zhou, H.-C. Wu, Y.-Q. Bie, Z.-M. Liao and D.-P. Yu, *Nature communications*, 2013, 4, 1921.

24. M. Julliere, *Phys Lett A*, 1975, 54, 225-226.

25. G.-X. Miao, M. Münzenberg and J. S. Moodera, *Reports on Progress in Physics*, 2011, 74, 036501.
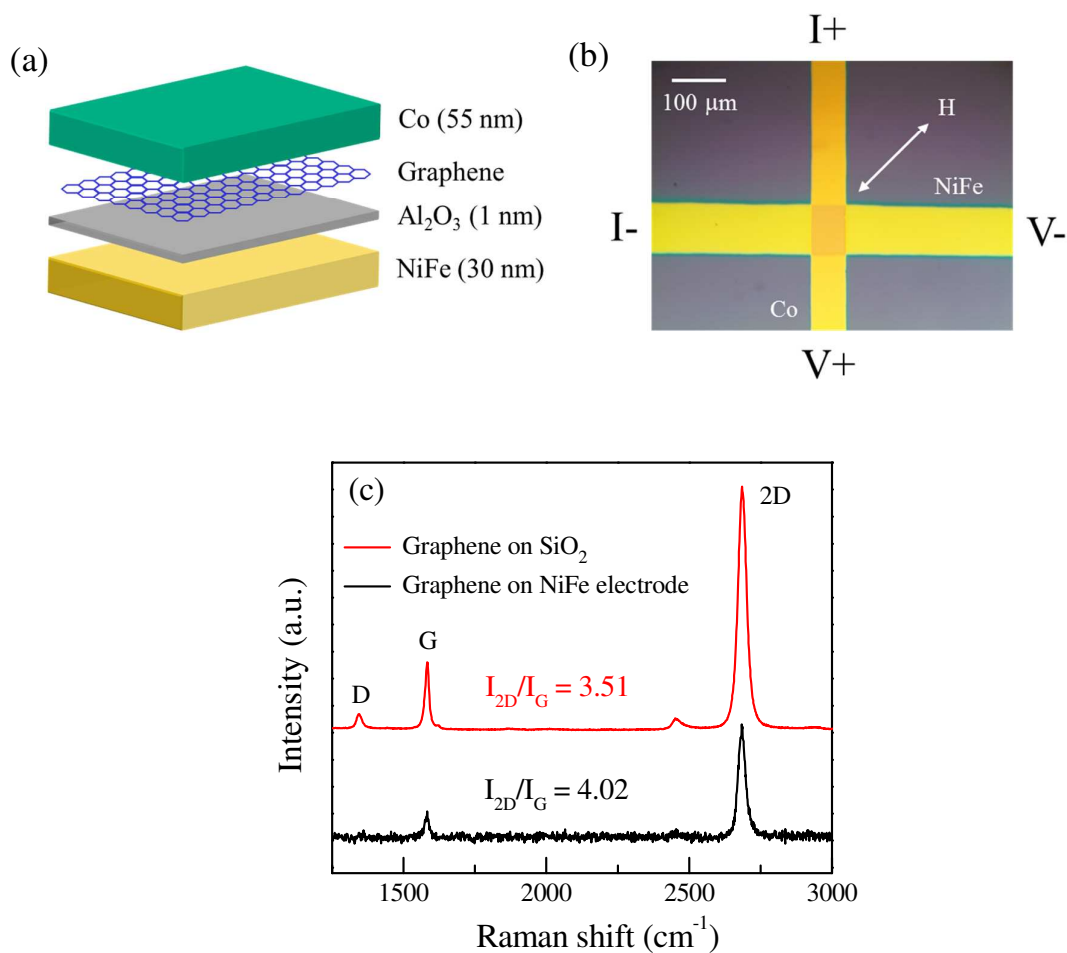
Figure 1. (a) Schematic of graphene/Al$_2$O$_3$ spin valve consisting of a top Co electrode (FM1), a bottom NiFe electrode (FM2) with an Al$_2$O$_3$ and graphene interlayer. Both the graphene interlayer and the Al$_2$O$_3$ film can be used separately. (b) Optical micrograph of the NiFe/Al$_2$O$_3$/graphene/Co junction. The bottom NiFe electrode is 100 μm wide and 30 nm thick, and the top Co electrode is 70 μm wide and 55 nm thick. (c) Raman spectra of CVD-grown graphene transferred on the NiFe electrode and SiO$_2$ substrate.
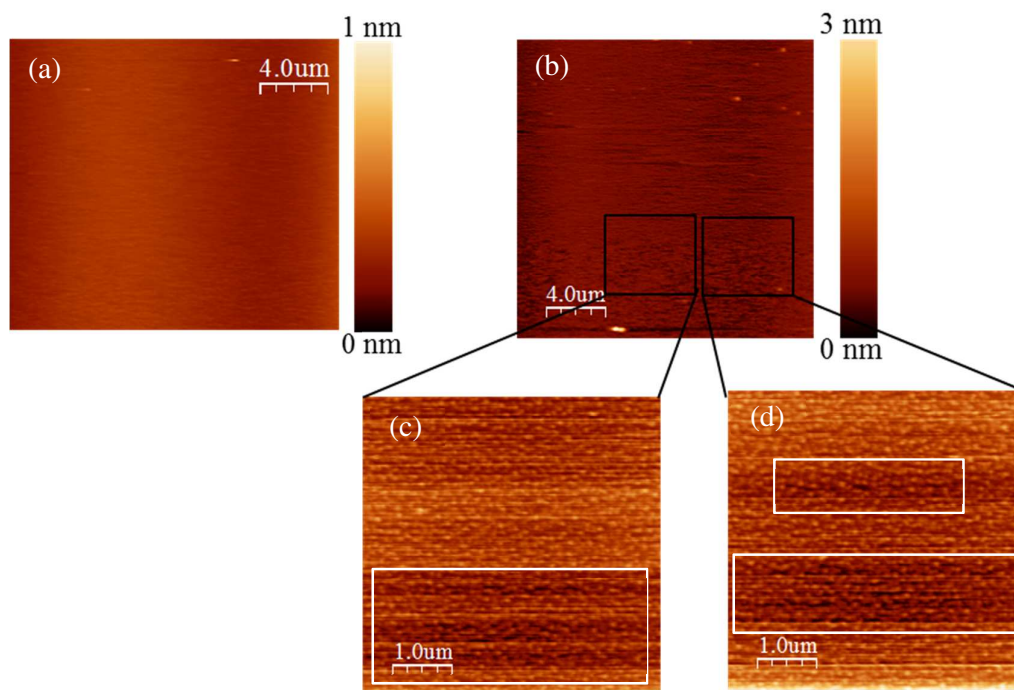
Figure 2. (a) AFM image of NiFe electrode before Al₂O₃ deposition. (b) AFM image of NiFe electrode after Al₂O₃ deposition. (c, d) The topography of the specified areas of NiFe electrode after Al₂O₃ deposition for clarity.
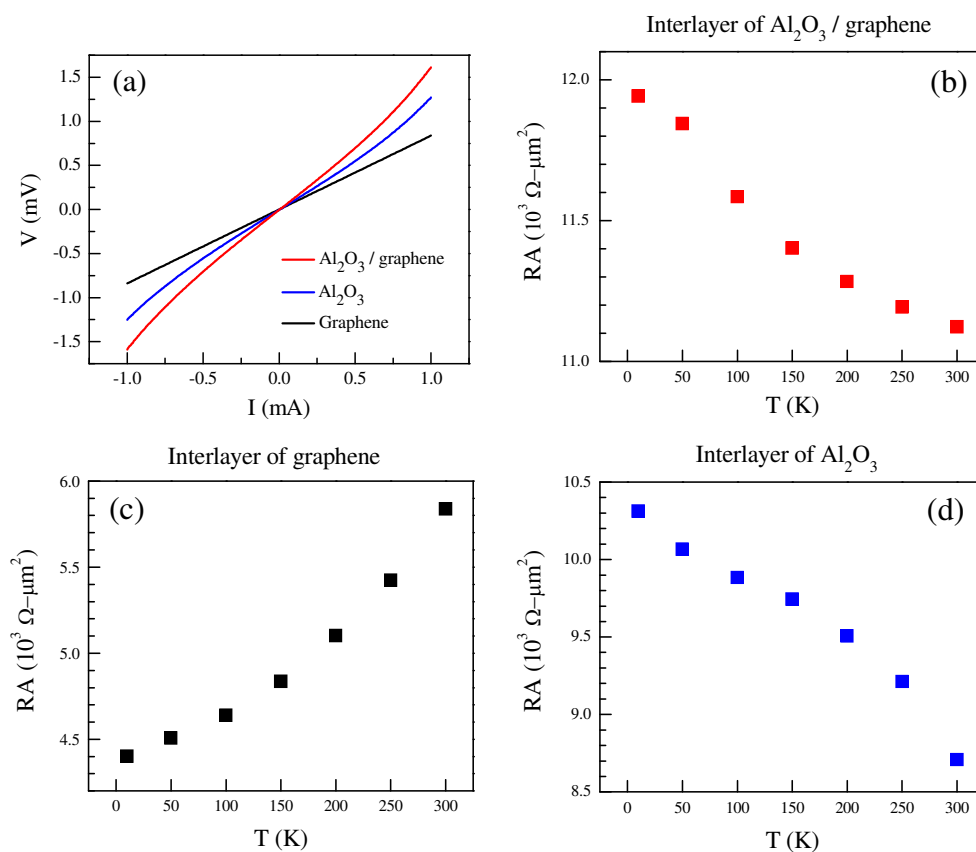
Figure 3. (a) I–V characteristics of the Al_2O_3/graphene, Al_2O_3, and graphene interlayer junctions. The graphene interlayer device (black line) presents a linear behavior indicative of Ohmic properties, the Al_2O_3/graphene (red line) or Al_2O_3 (blue line) interlayer junction show nonlinear curves corresponding with tunneling characteristics. (b) Resistance-area product (RA) as a function of temperature for the Al_2O_3/graphene interlayer junction. The resistance decreases monotonically as temperature increases from 10 K to 300 K. (c) RA as a function of temperature for the graphene interlayer junction. The resistance increases monotonically as

15

temperature increases. (d) RA as a function of temperature for the Al_2O_3 interlayer junction.

The junction resistance decreases as temperature increases.

Interlayer of Al_2O_3 / graphene

(a)

300 K
250 K
200 K
150 K
100 K
50 K
10 K

Interlayer of graphene

(b)

300 K
250 K
200 K
150 K
100 K
50 K
10 K

Interlayer of Al_2O_3

(c)

300 K
250 K
200 K
150 K
100 K
50 K
10 K
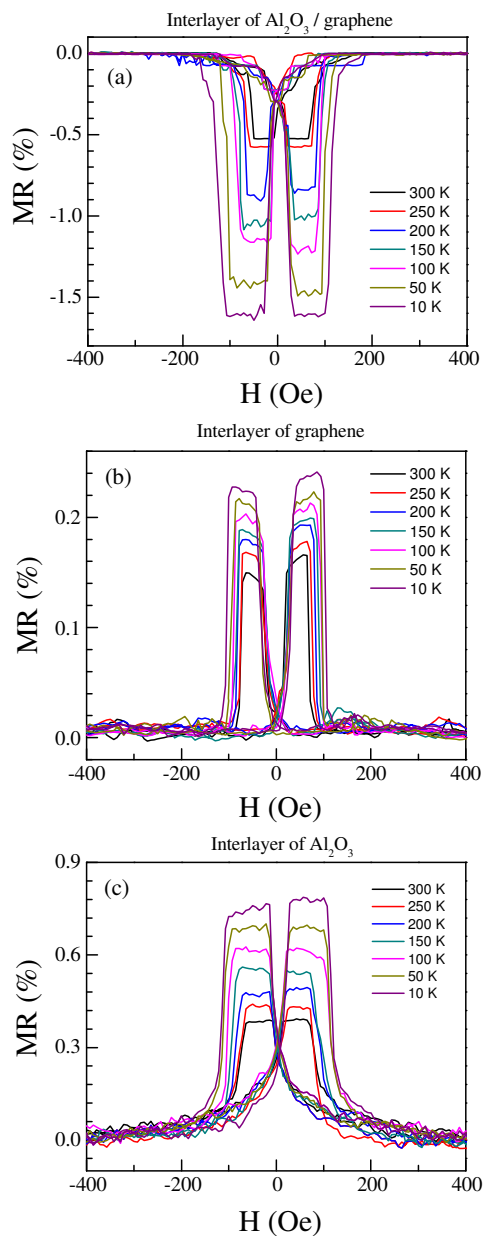
Figure 4. (a) MR ratio of the Al_2O_3/graphene interlayer spin valve from 10 K to 300 K. The

negative MR value is observed for the antiparallel magnetization configuration between FM1

and FM2. (b) MR ratio of the graphene interlayer spin valve from 10 K to 300 K. A positive

MR value is observed. (c) MR ratio of the Al_2O_3 interlayer spin valve from 10 K to 300 K. A

positive MR value is observed.

TABLE OF CONTENTS

Interlayer dependent polarity of magnetoresistance in graphene spin valves

M. Z. Iqbal, M. W. Iqbal, Xiaozhan Jin, Changyong Hwang, Jonghwa Eom

We have studied the polarity of magnetoresistance (MR) in three types of magnetic junction. While the NiFe/single layer graphene (SLG)/Co and NiFe/Al$_2$O$_3$/Co junctions showed spin valve signals with positive MR, the NiFe/Al$_2$O$_3$/SLG/Co junction revealed negative MR values.